

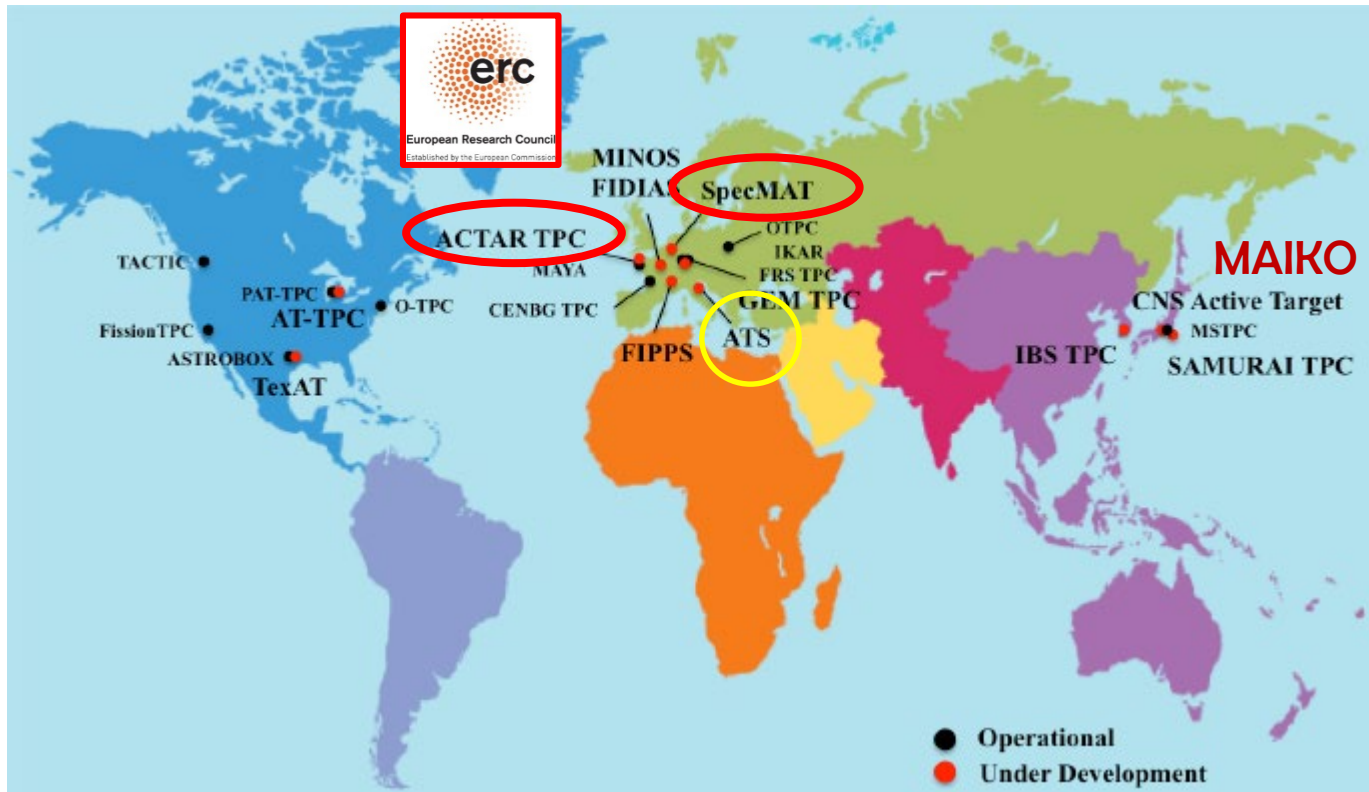
Actar Demonstrator test at LNS: an overview

“Performance test and optimization of the ACTAR Demonstrator for heavy ion beams experiments.”

GDS Workshop
on Rare gas target handling and recycling systems
Orsay, 23/01/2019

T. Marchi INFN – LNL

Active Targets around the World



G.F. Grinyer, J. Pancin, T. Roger, EURISOL meeting 2014

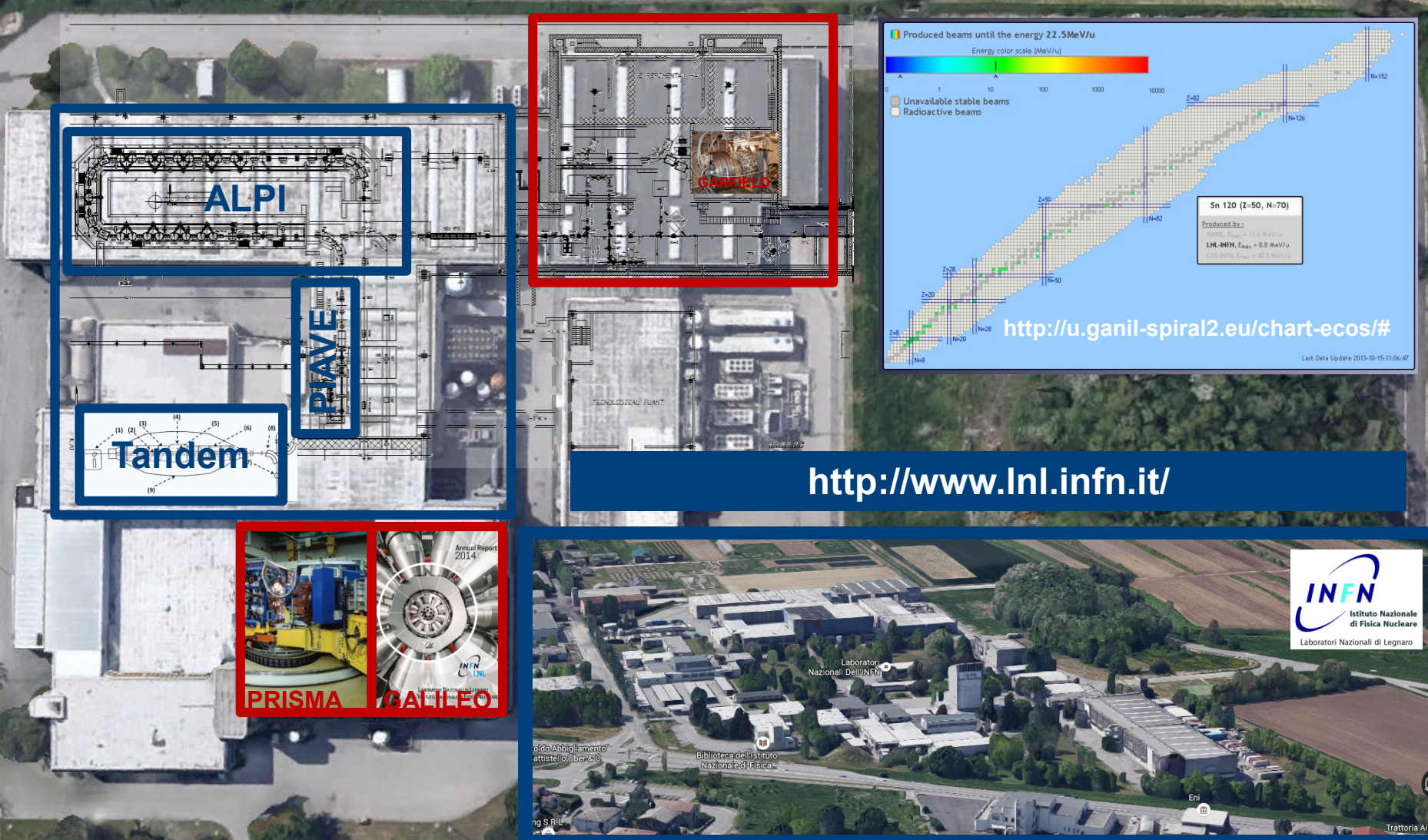
Review about Active Target detectors:

S. Beceiro-Novo, T.Ahn, D. Bazin, W. Mittig, Prog. in Part. & Nucl. Physics (2015) 124- 165,

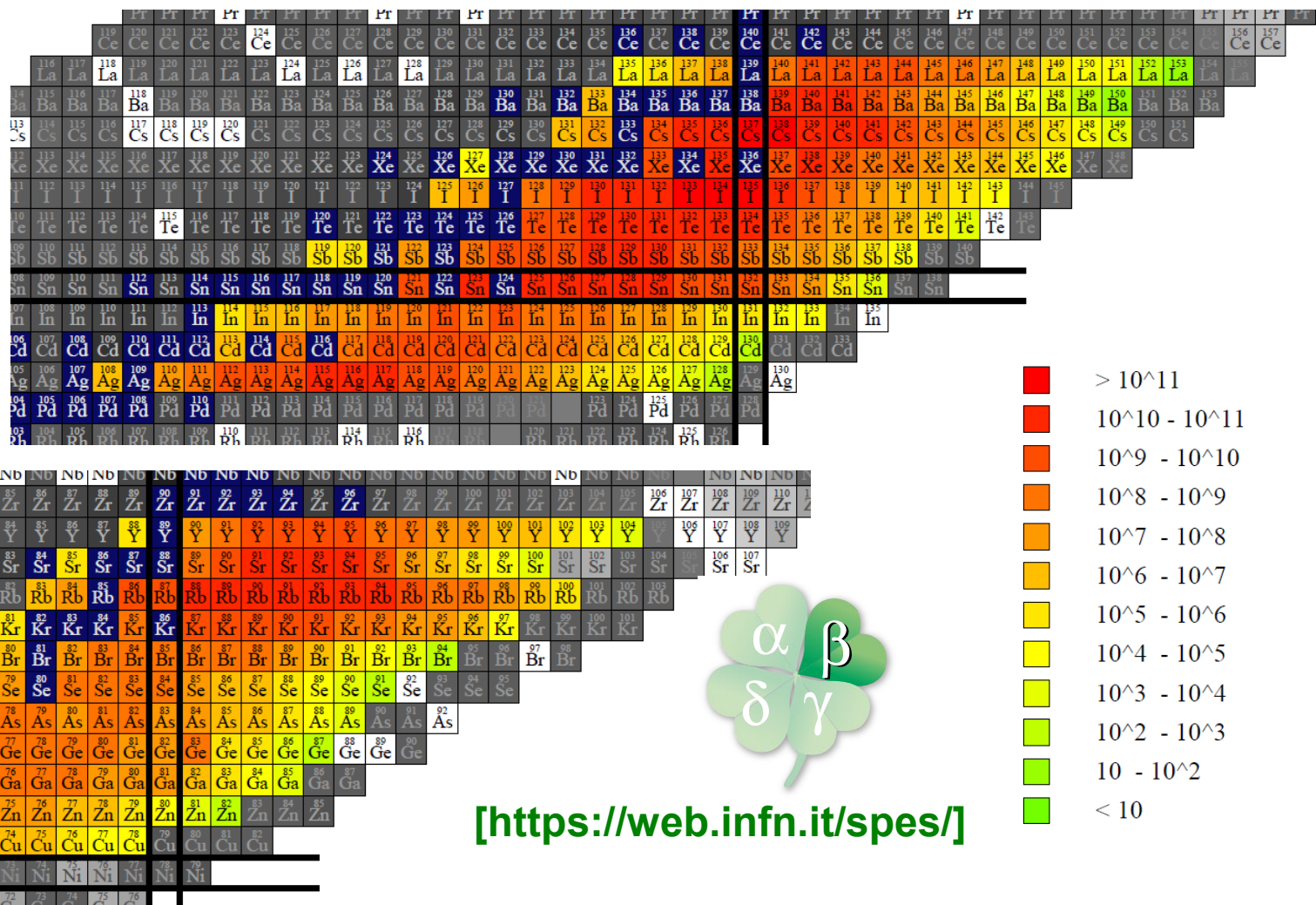
Outline

- An Active Target for SPES, exploiting the ACTAR TPC Demonstrator
- ACTAR-test campaign at LNS (December 2018 - February 2019)
- Next steps with the ACTAR Demonstrator

An Active Target for SPES- β



SPES beams



[<https://web.infn.it/spes/>]

Two letters of intent for SPES endorsed by the SAC:

- B. Fernandez Dominguez et al, Direct Reactions with exotic nuclei in the r-process using an active target
 R. Raabe, T. Marchi et al, Shell Structure in the vicinity of ^{132}Sn with an active target

$f_{7/2}$ vs $p_{3/2}$ neutron orbitals, in Sn like in Ca?

MagicTin*

	134Te 41.8 M	135Te 19.0 S	136Te 17.63 S	137Te 2.49 S	138Te 1.4 S	139Te >150 NS	140Te >300 NS	141Te >150 NS	142Te
51	β^- : 100.00%	β^- : 100.00%	β^- : 100.00% β^-n : 1.31%	β^- : 100.00% β^-n : 2.99%	β^- : 100.00% β^-n : 6.30%	β^-n	β^-n	β^-n	
	133Sb 2.34 M	134Sb 0.78 S	135Sb 1.679 S	136Sb 0.923 S	137Sb 492 MS	138Sb 350 MS	139Sb 93 MS	140Sb >407 NS	
50	132Sn 39.7 S	133Sn 1.46 S	134Sn 1.050 S	135Sn 530 MS	136Sn 0.25 S	137Sn 190 MS	138Sn >408 NS		
	β^- : 100.00%	β^- : 100.00% β^-n : 22.00%	β^- : 100.00% β^-n : 16.30%	β^- : 100.00% β^-n : 49.00%	β^- : 100.00% β^-n : 72.00%	β^- : 100.00% β^-n : 90.00%	β^-n	β^-n	
49	131In 0.28 S	132In 0.207 S	133In 165 MS	134In 140 MS	135In 92 MS				
	β^- : 100.00% β^-n : 2.00%	β^- : 100.00% β^-n : 6.30%	β^- : 100.00% β^-n : 17.00%	β^- : 100.00% β^-n : 21.00%	β^- : 100.00% β^-n : 30.00%	β^- : 100.00% β^-n : 58.00%	β^-n	β^-n	
48	130Cd 162 MS	131Cd 68 MS	132Cd 97 MS	133Cd 57 MS					
	β^- : 100.00% β^-n : 3.50%	β^- : 100.00% β^-n : 3.50%	β^- : 100.00% β^-n : 60.00%	β^- : 100.00% β^-n					
	82	83	84	85	86	87	88		
	N=82								

[Adapted from O. Sorlin, M.-G. Porquet,
Progr Part. Nucl Phys 61 (2008) 602]

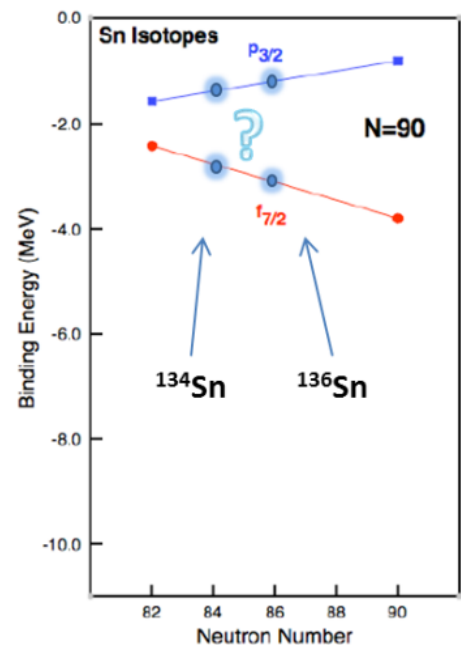
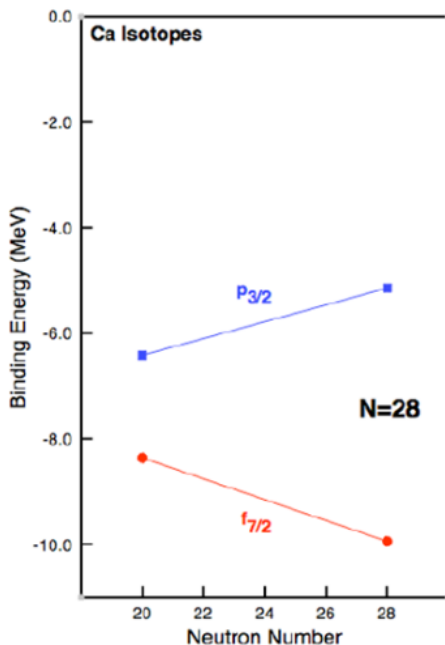


Fig.1 Analogy between $f_{7/2}$ and $p_{3/2}$ evolution of binding energies in the known Ca isotopes to what could be expected for the Sn isotopes approaching $N=90$. Figure adapted from¹³.

Lol endorsed by SPES SAC

typical physics case

Beyond ^{132}Sn

(11/2-) ————— 3700

(5/2-) ————— 2004.6

(9/2-) ————— 1560.9

(1/2-) ————— 1363

3/2- ————— 853.7

7/2- ————— 0.0 1.46 S

^{133}Sn

$d(^{132}\text{Sn}, ^{133}\text{Sn})p$
Q = 177 keV

(8+) ————— 2508.9

6+ ————— 1247.4 80 N!

4+ ————— 1073.4

2+ ————— 725.6

0+ ————— 0.0 1.050 S

(7/2-) ————— 0.530 MS

^{134}Sn

$d(^{133}\text{Sn}, ^{134}\text{Sn})p$
 $Q_{\text{gs}} = 1.4 \text{ MeV}$

^{135}Sn

$d(^{134}\text{Sn}, ^{135}\text{Sn})p$
Q = 47 keV

Expected beam intensities @ 10 AMeV

	SPES 1 st day (5 μA p beam)	SPES full power (200 μA p beam)
^{132}Sn	7.8 10⁵	3.1 10⁷
^{133}Sn	7.0 10⁴	2.8 10⁶
^{134}Sn	1.2 10⁴	4.9 10⁵
^{135}Sn	1.6 10²	6.2 10³
^{136}Sn	-	0.9 10²

Band 1

(6+) ————— 1295 46 N

(4+) ————— 1079

(2+) ————— 688

0+ ————— 0.0 290 S

0 190 MS

^{137}Sn

$d(^{136}\text{Sn}, ^{137}\text{Sn})p$
Q = -264 keV

(6+) ————— 1344 210

(4+) ————— 1176

(2+) ————— 715

0+ ————— 0.140 MS

^{138}Sn

$d(^{137}\text{Sn}, ^{138}\text{Sn})p$
Q = 0.9 MeV

The ACTAR TPC Demonstrator

Active Volume: **6,4 x 12,8 x 17,0 cm³**

Total Gas Volume: **about 10 l**

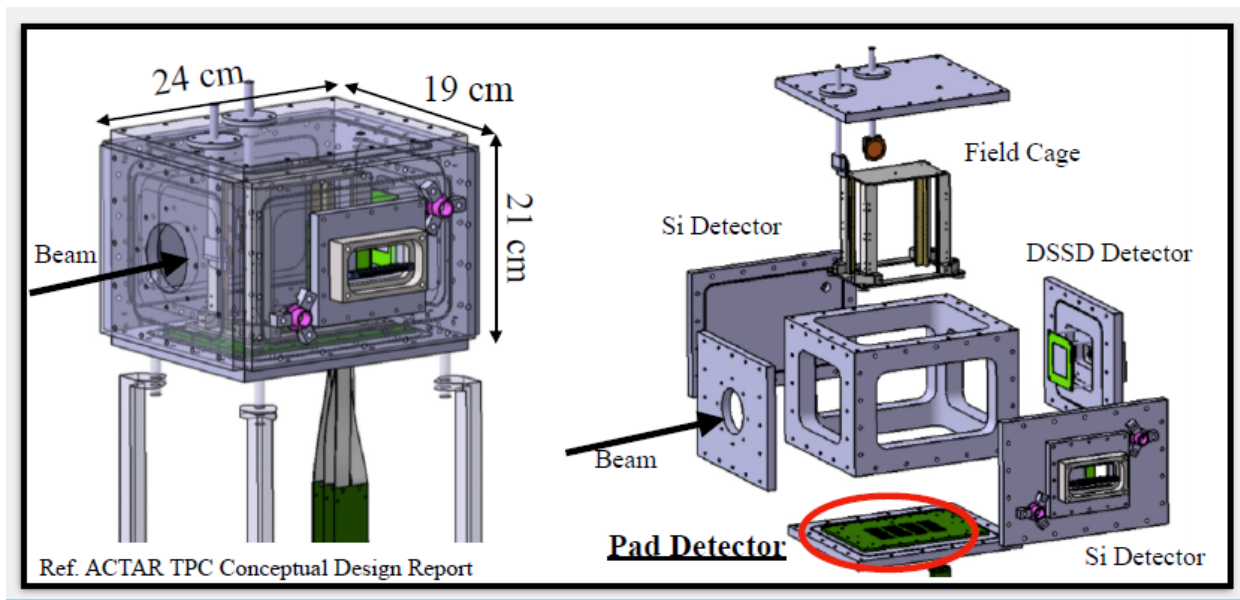
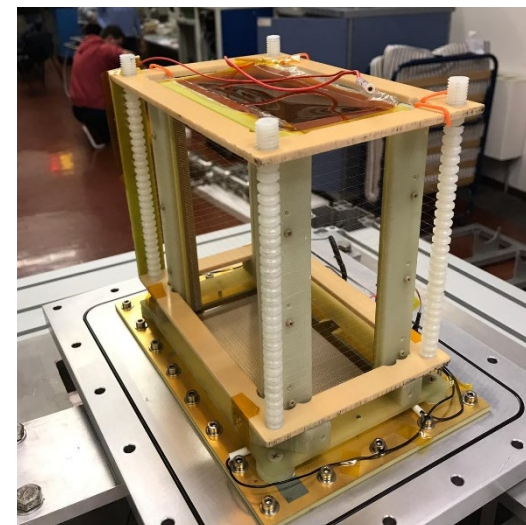
Operating pressure: **0-2 bar**

Maximum Cathode Voltage: **3kV**

MPGA: micromegas (**220 μm gap**)

Charge collection: **2048 pads - 2x2 mm²**

Beam interface: **6μm MYLAR window**



ACTAR TPC Demonstrator at IPNO 2015

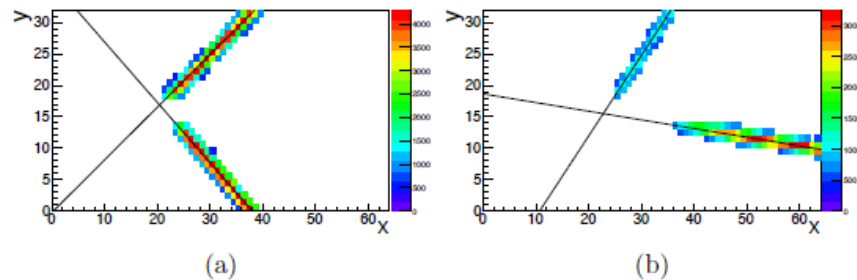
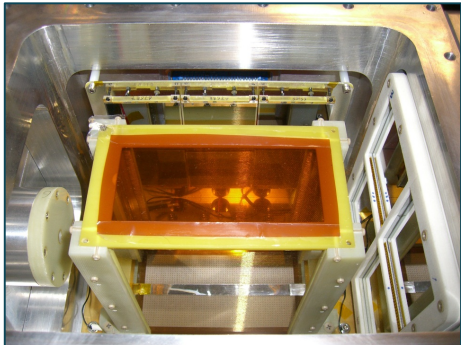
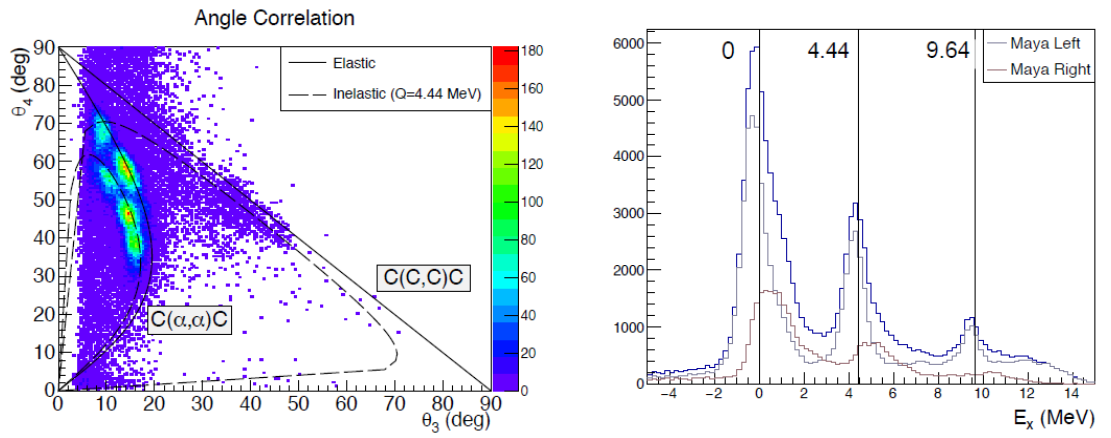
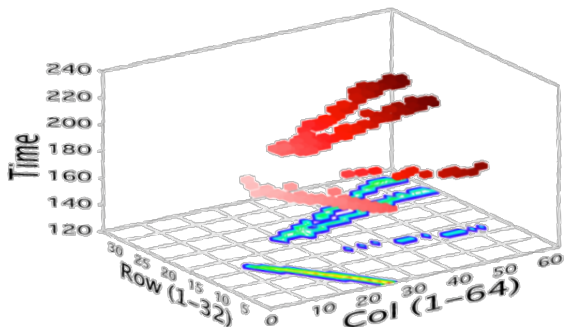


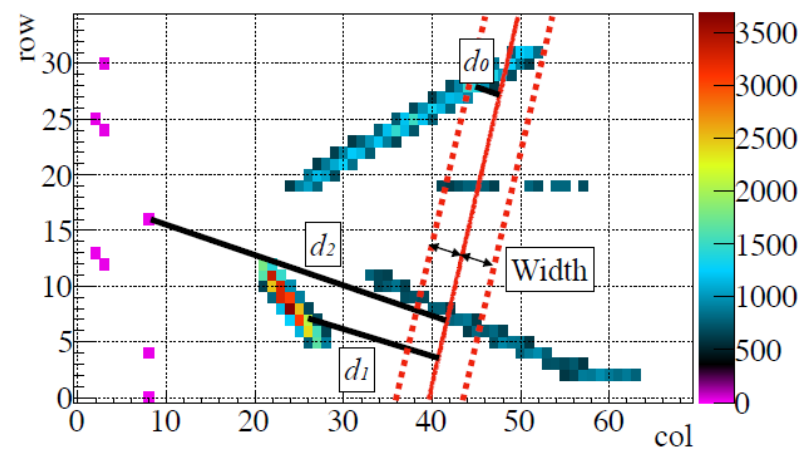
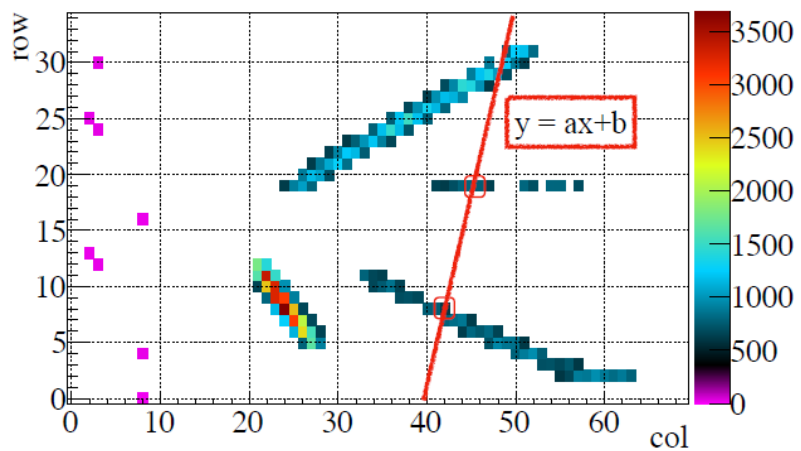
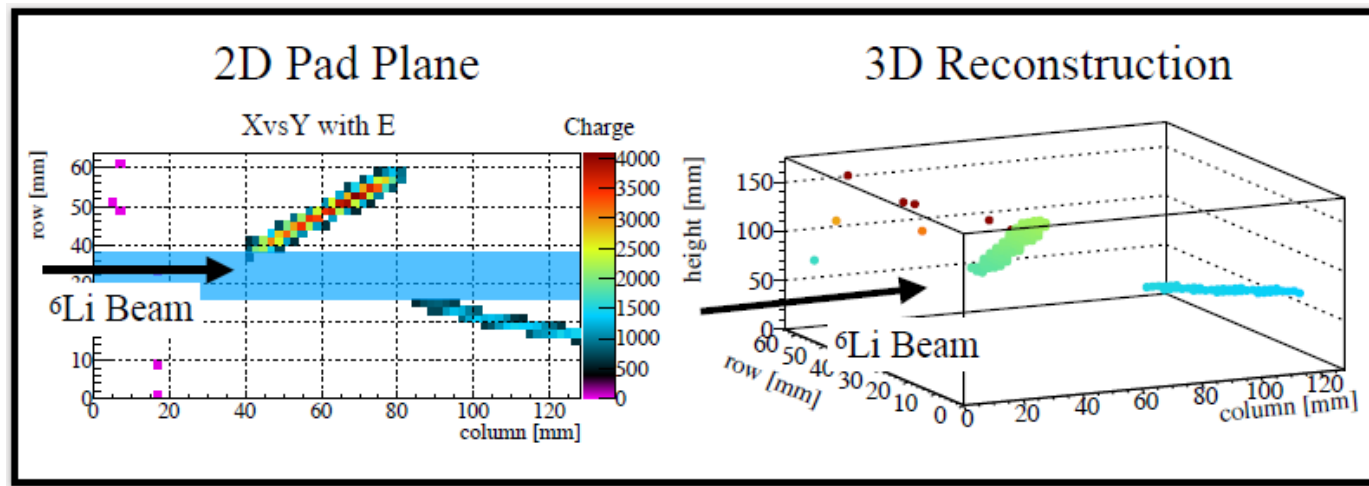
Figure 4.19: Charge deposition on the pad plane of (a) a $^{12}\text{C}(^{12}\text{C},^{12}\text{C})^{12}\text{C}$ and (b) a $^{12}\text{C}(\alpha,\alpha)^{12}\text{C}$ scattering reaction.



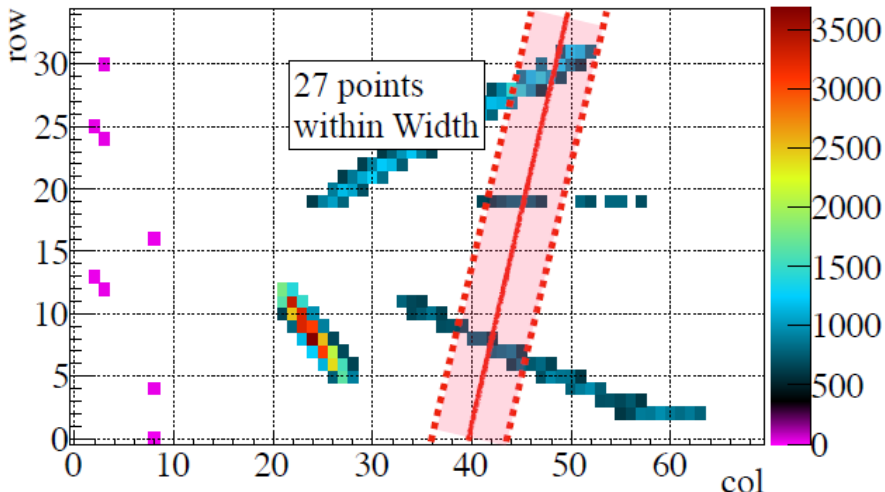
^{12}C @80 MeV on He: C_4H_{10} (90:10)
 ^{6}Li @11-20 MeV on He: CO_2 (90:10)

Main issues:
Non homogeneous electric field
Zero suppression thresholds
Gas composition

PID and Tracking



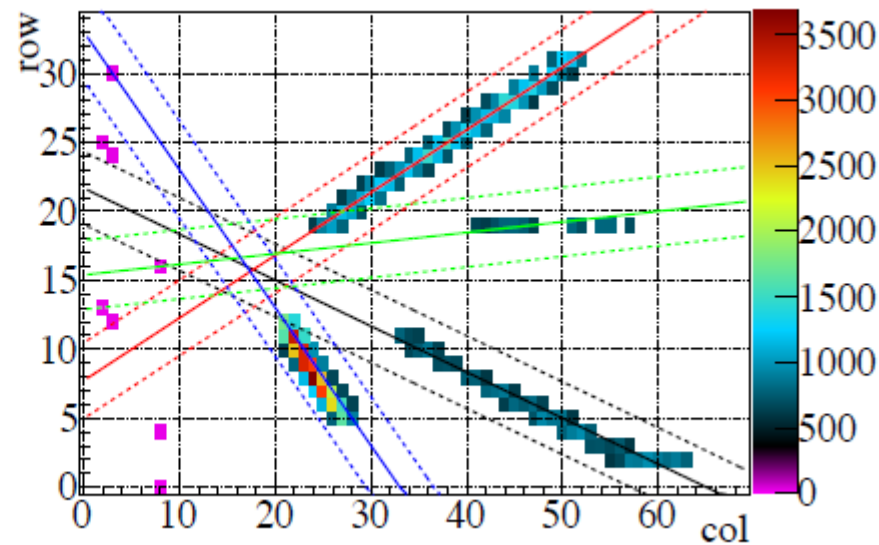
PID and Tracking



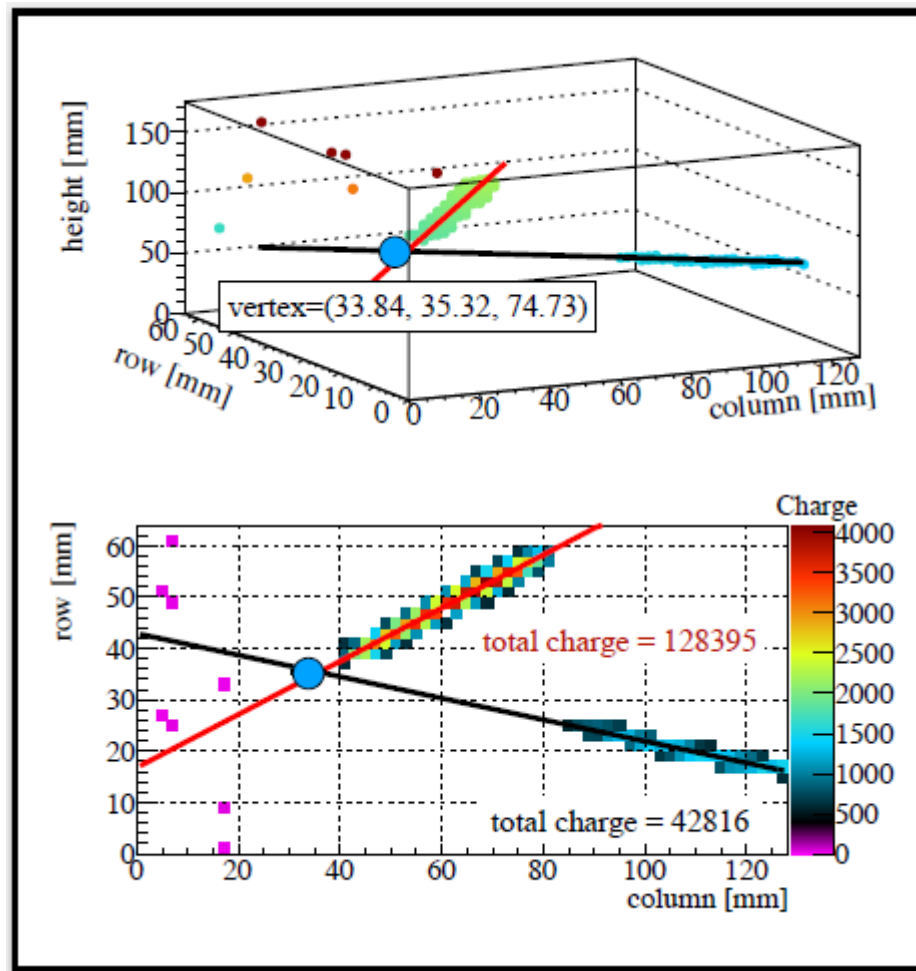
Run #205, event #5	
Max Loop	7500
Length	10
Width	2.5

$$\text{Mean} = \frac{\sum d_i}{\text{number of elements}}$$

Minimize «Mean» to obtain the track «clusters», then fit linear trajectories



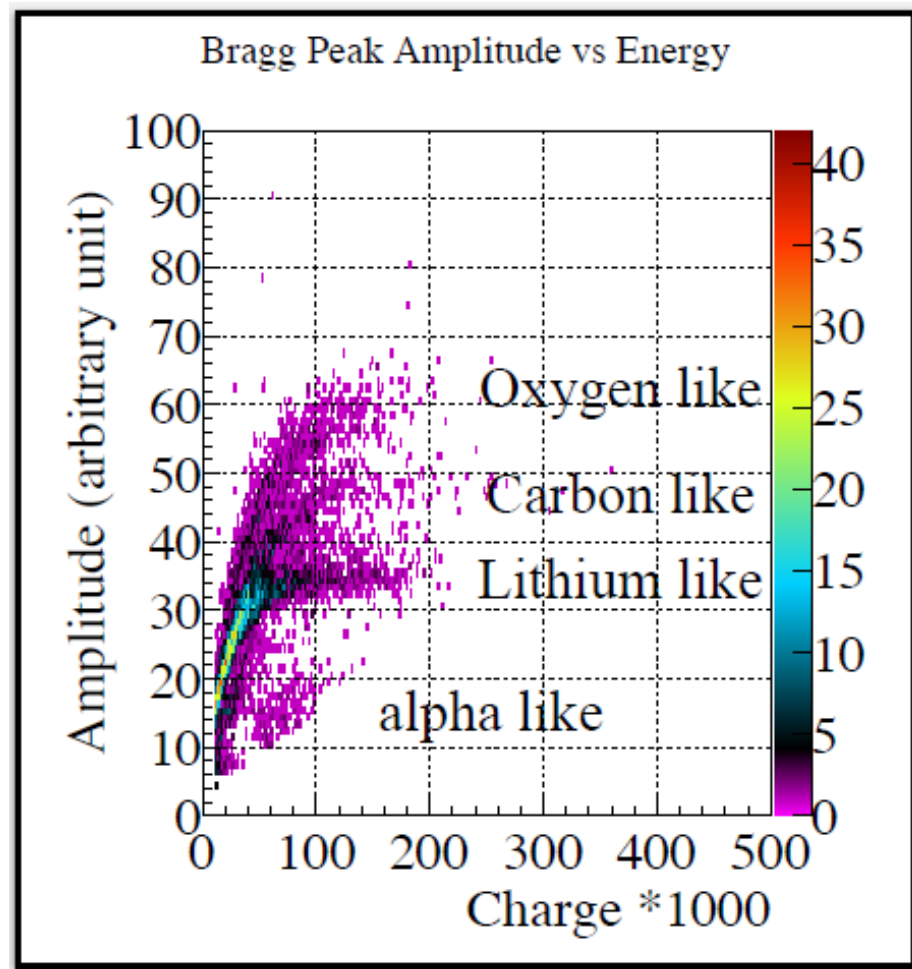
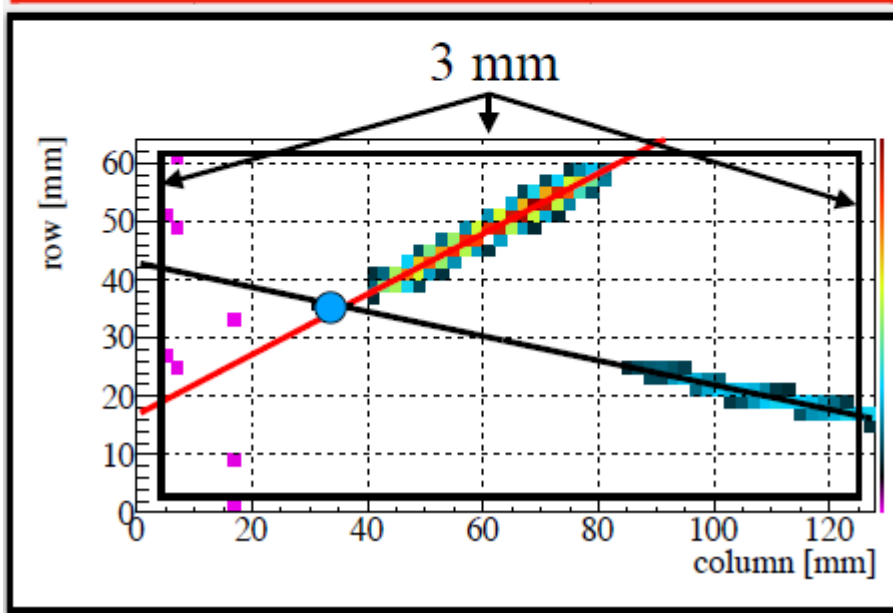
PID and Tracking



	Number of Event	Ratio (Track/Total Event)
1 Track	10580	16.9%
2 Tracks	39461	63.1%
3 Tracks	9487	15.2%
4 Tracks	478	0.8%

PID and Tracking

Event Selection		
Cut 1	Event has 2 tracks	Track Fitting
Cut 2	Vertex position is in beam region	Vertex Fitting
Cut 3	A particle stops inside the gas volume	Pad Information



Next steps

- 1. The ‘new’ setup at LNL**
- 2. Validation of the experimental techniques**
- 3. Charachterization of the response to heavy ions**

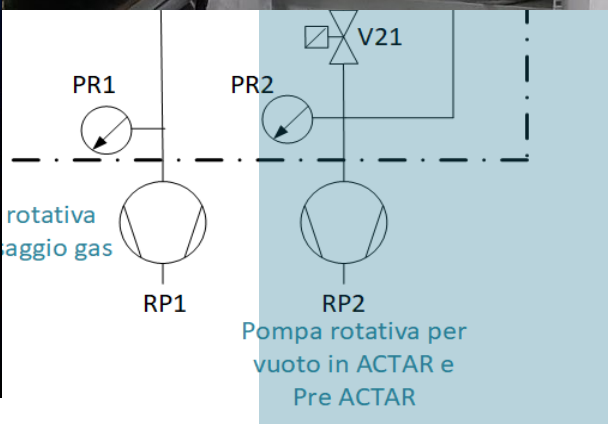
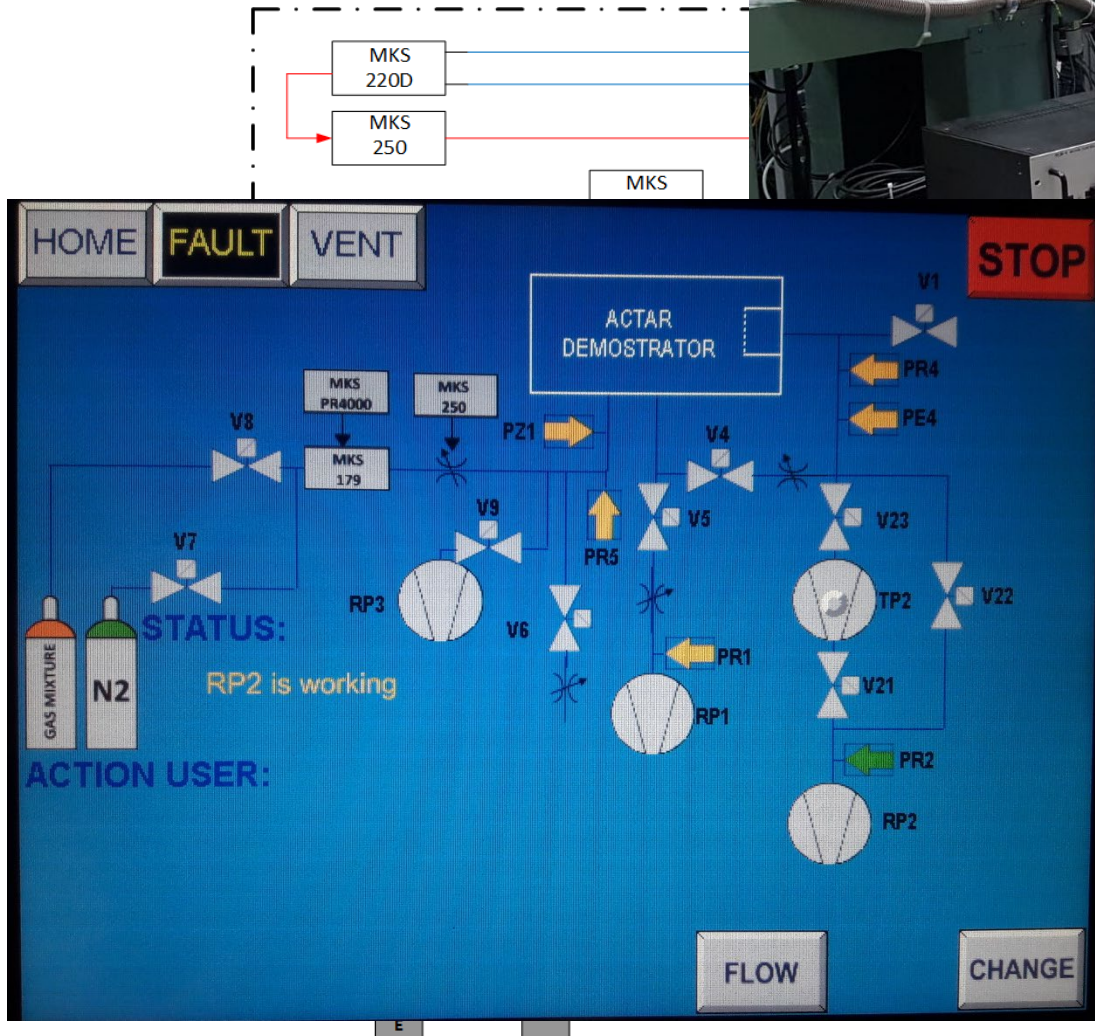
The GAS system

Design constraints:

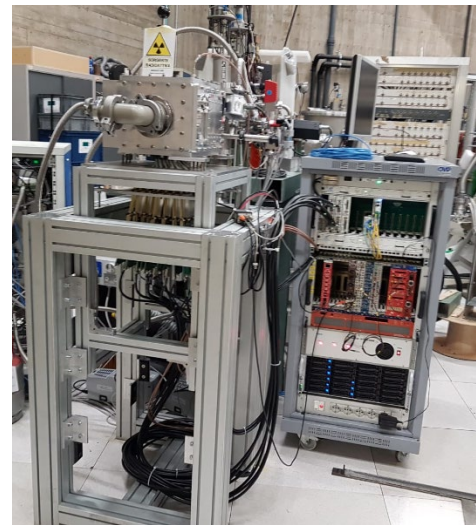
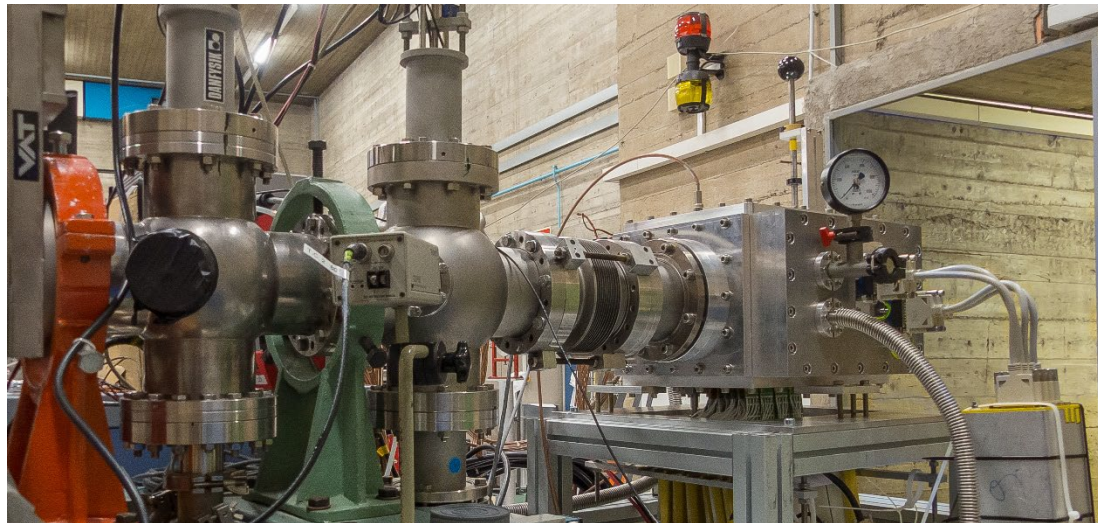
- 1- Hazards: explosive, flammable, toxic, polluting gases
- 2- Pressure gauge calibration can be gas dependent
- 3- Exhaust management
- 4- Easy to operate and to move
- 5- Remotely controllable (plus pressure value storing in the data stream)
- 6- Stable and fast in pressure control
- 7- Ensure window safety
- 8- *MIXING is not always simple, rather buy pre-mixed bottles*

CERTIFICATION according to local regulation

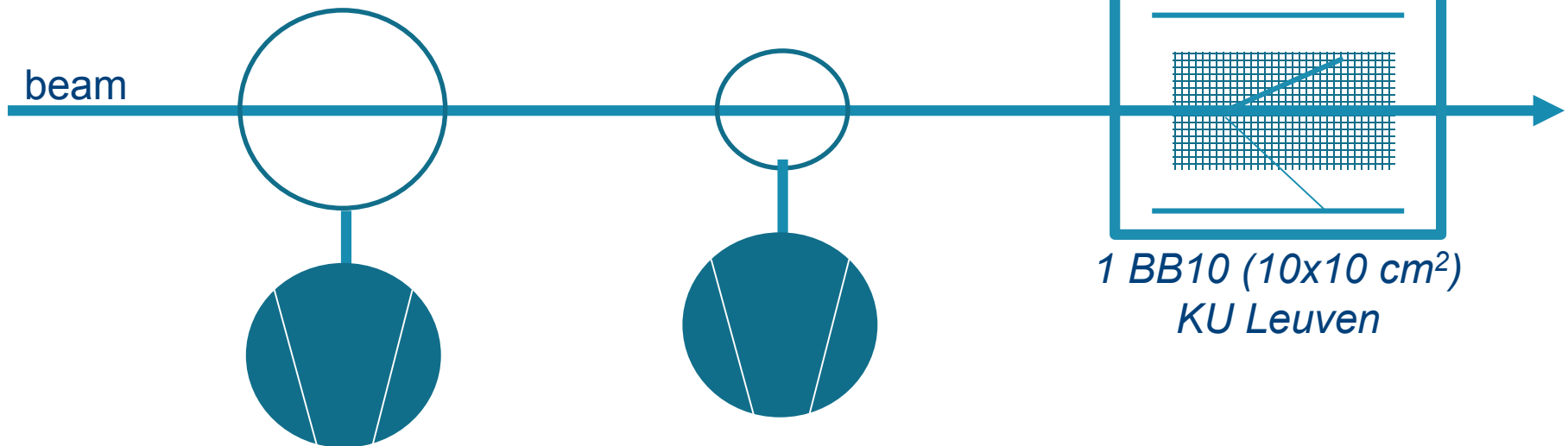
The GAS system



ACTARtest at LNS - setup



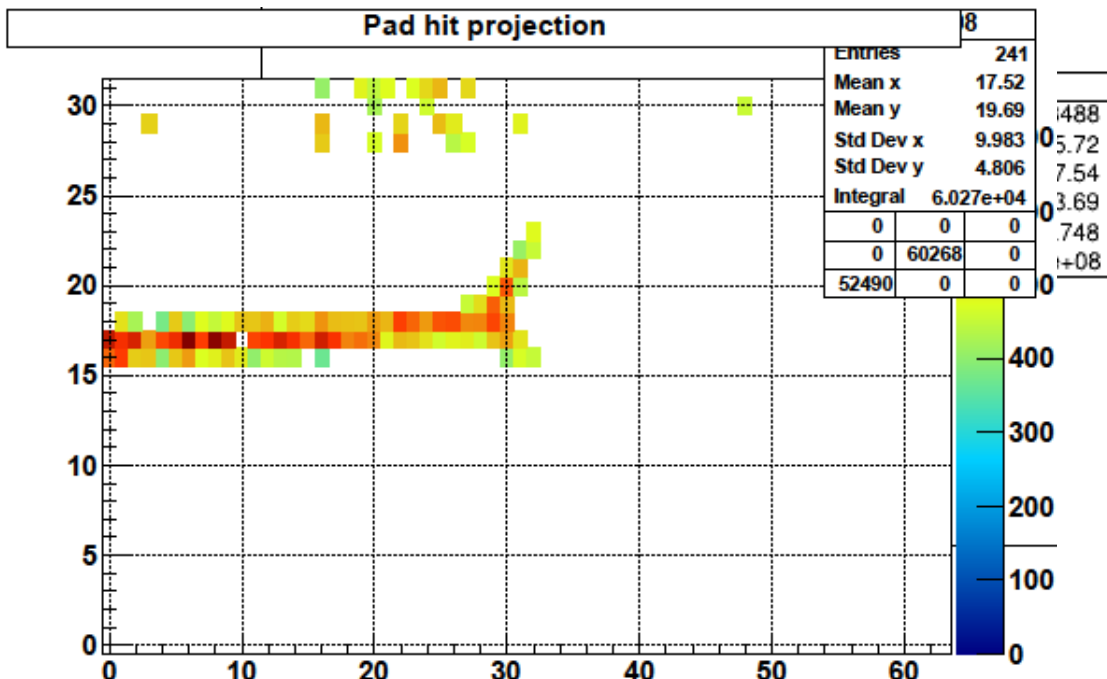
Using GET electronics



ACTARtest at LNS – energy loss

beam	energy
p	3 MeV
^6Li ^7Li	7 – 9 MeV
^{10}B ^{11}B	30 - 33 MeV
^{12}C	36 MeV
^{14}N	42 MeV
^{16}O	45 MeV
^{27}Al	75 MeV
^{50}Ti	142 MeV
^{107}Ag	169 MeV

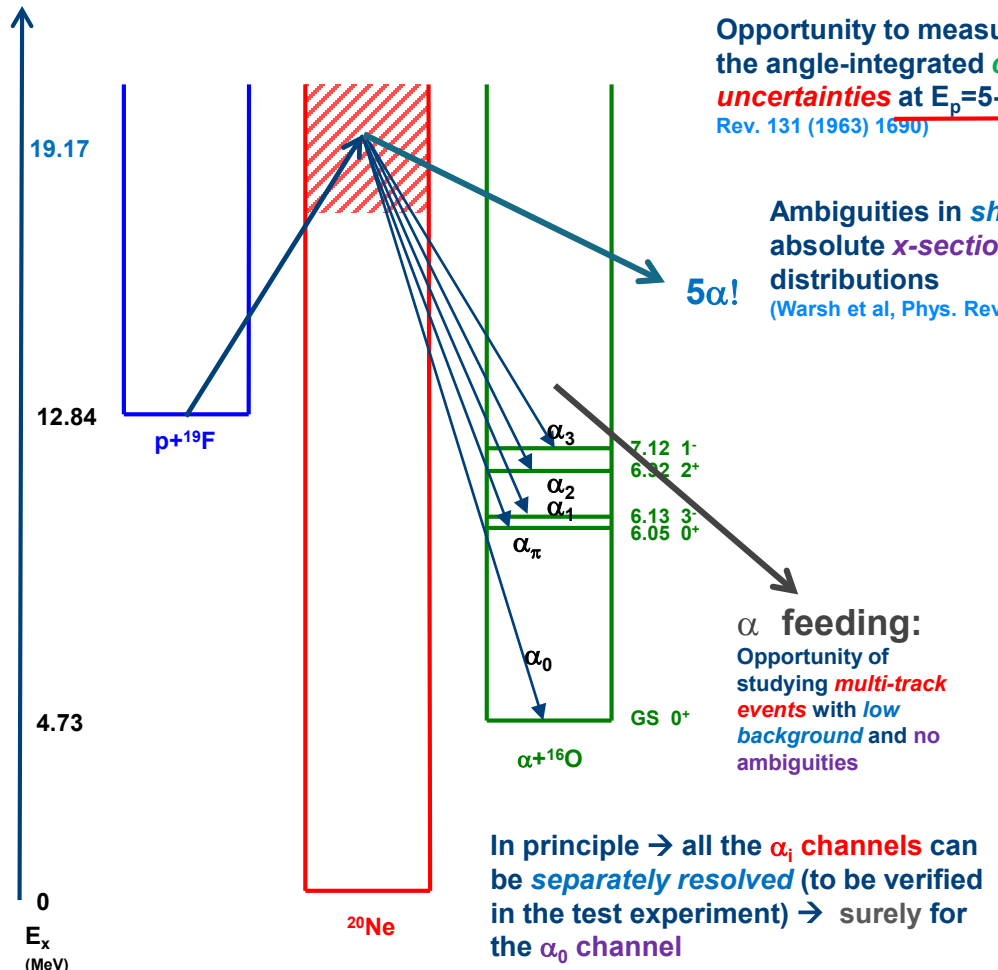
On different gases: CF4, iC4H10, CH4, P10, He:CO2



- 6 μm mylar window + dead layer
- ✓ Pressure tuned for full stopping
- ✓ External triggering using mesh signals
- ✓ Very low count rate to avoid pileup
- ✓ Multiple charge states measured for some cases (but still there is the window)

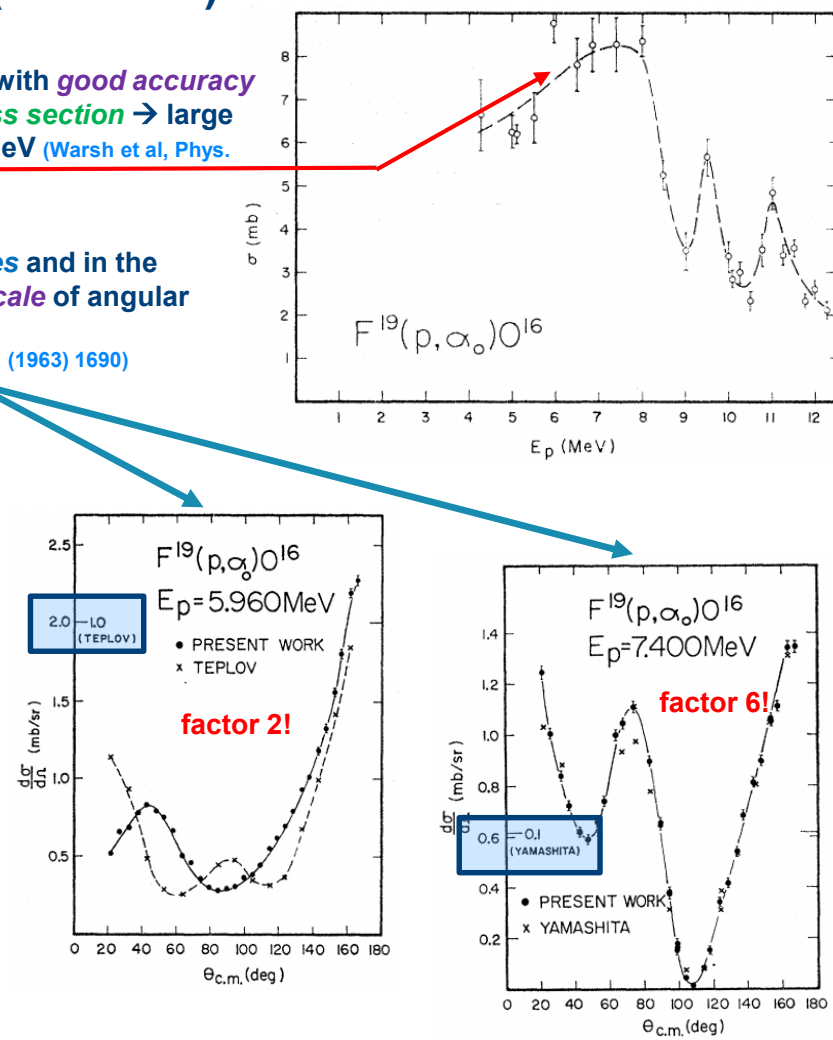
Actar test at Ins – reactions

Test case 1: $^{19}\text{F}(\text{p},\text{a})$ reaction at $E_{\text{p}}=5\text{-}7 \text{ MeV}$ (TANDEM)



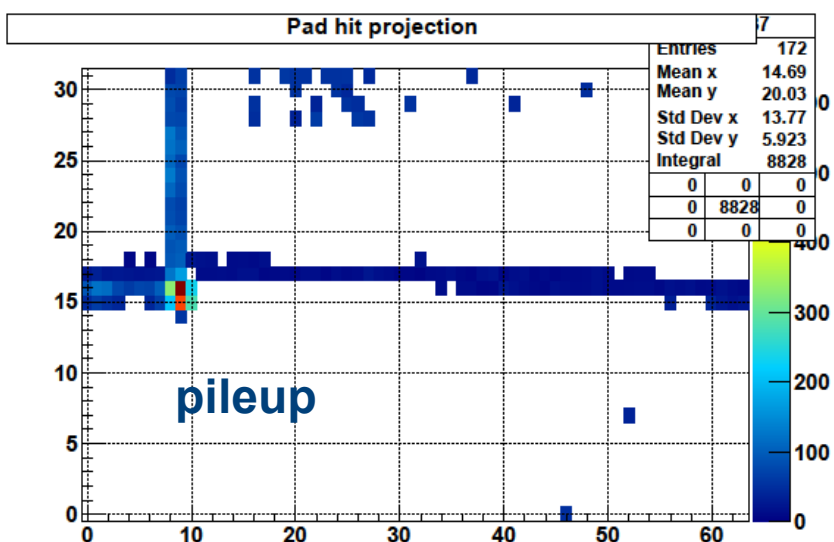
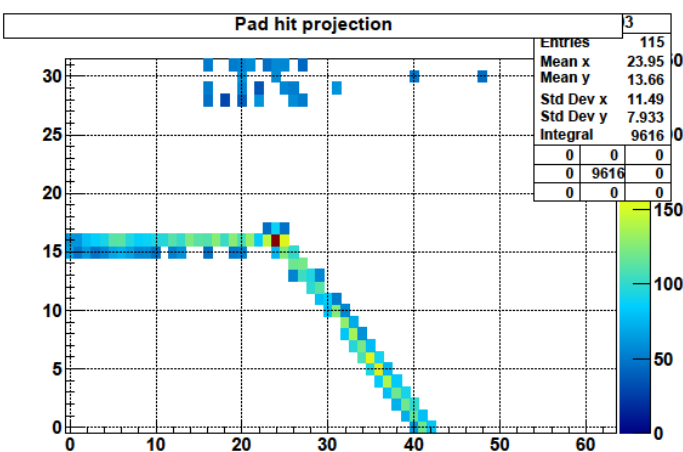
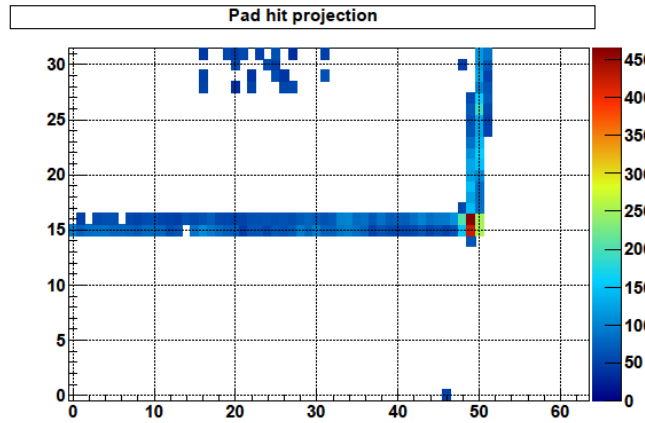
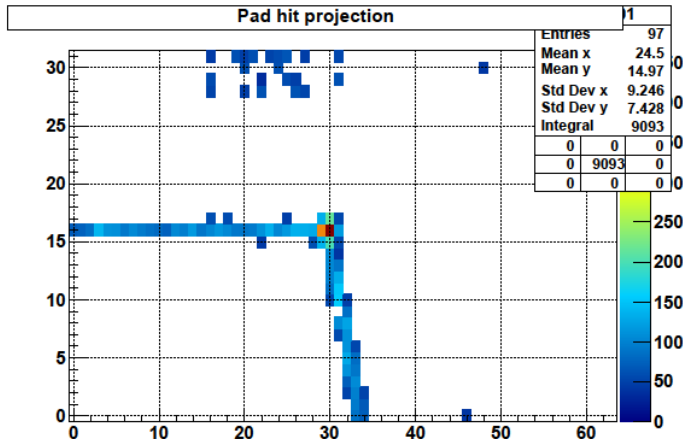
Opportunity to measure with *good accuracy* the angle-integrated *cross section* → large *uncertainties* at $E_{\text{p}}=5\text{-}7 \text{ MeV}$ (Warsh et al, Phys. Rev. 131 (1963) 1690)

Ambiguities in *shapes* and in the absolute *x-section scale* of angular distributions
(Warsh et al, Phys. Rev. 131 (1963) 1690)

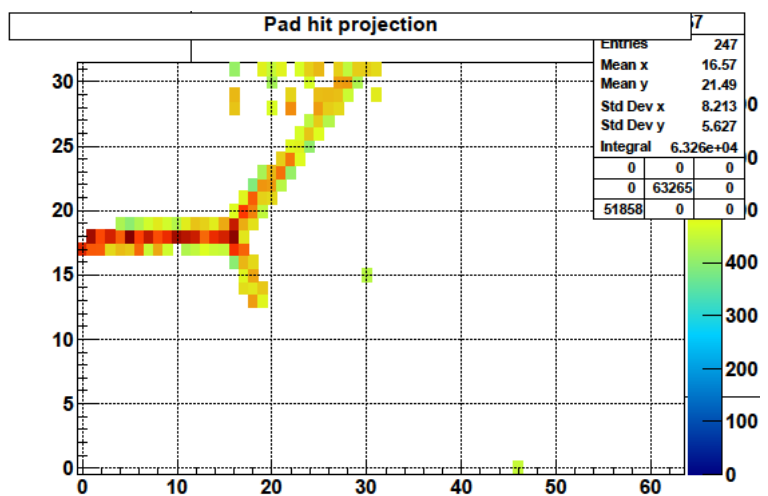


Actar test at Ins – reactions

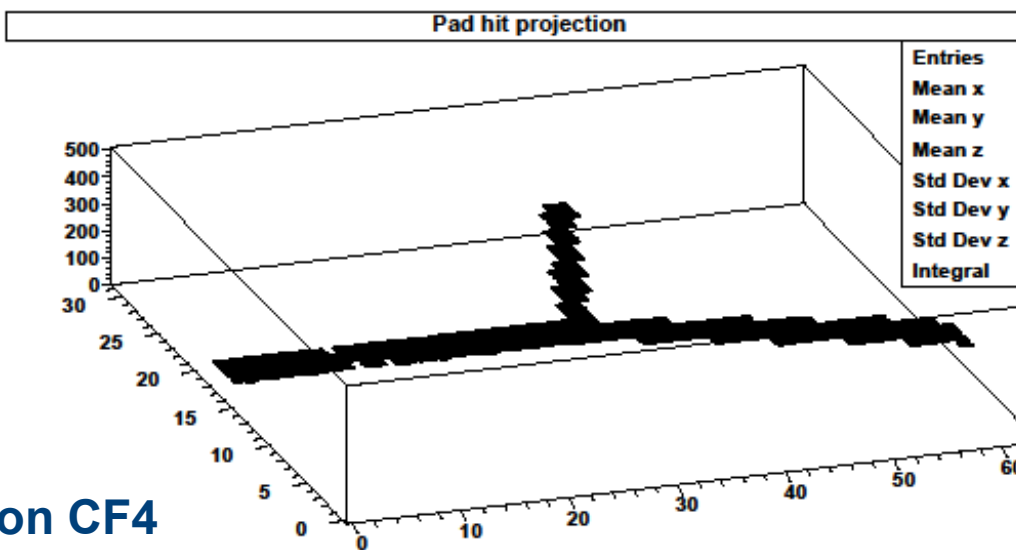
Test case 1: $^{19}\text{F}(\text{p},\text{a})$ reaction at $E_{\text{p}}=5\text{-}7 \text{ MeV}$ (TANDEM)



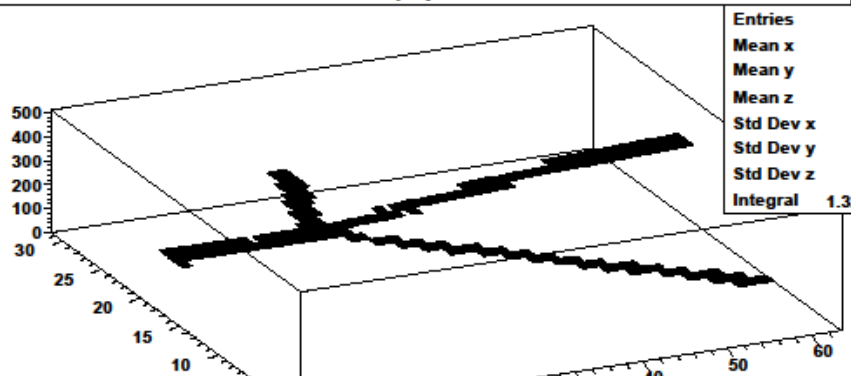
Actar test at Ins – reactions



^7Li on CF_4

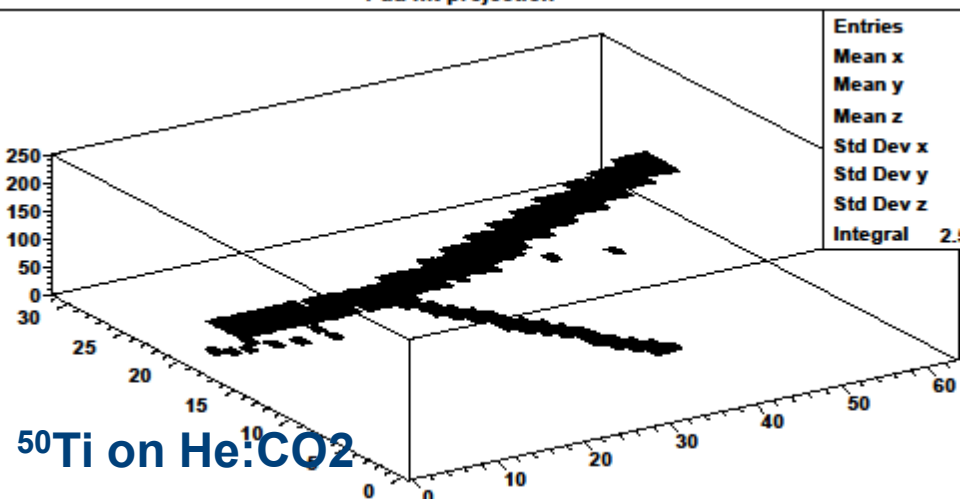


Pad hit projection



^{11}B on iC_4H_{10}

Pad hit projection



^{50}Ti on He:CO_2

NOTES for experiment's preparation

Projectile & Target

Energy of interest

Cross section/
Target Thickness

GAS

GAS
PRESSURE

Electric
fields

GAIN

Ejectile's
energy loss

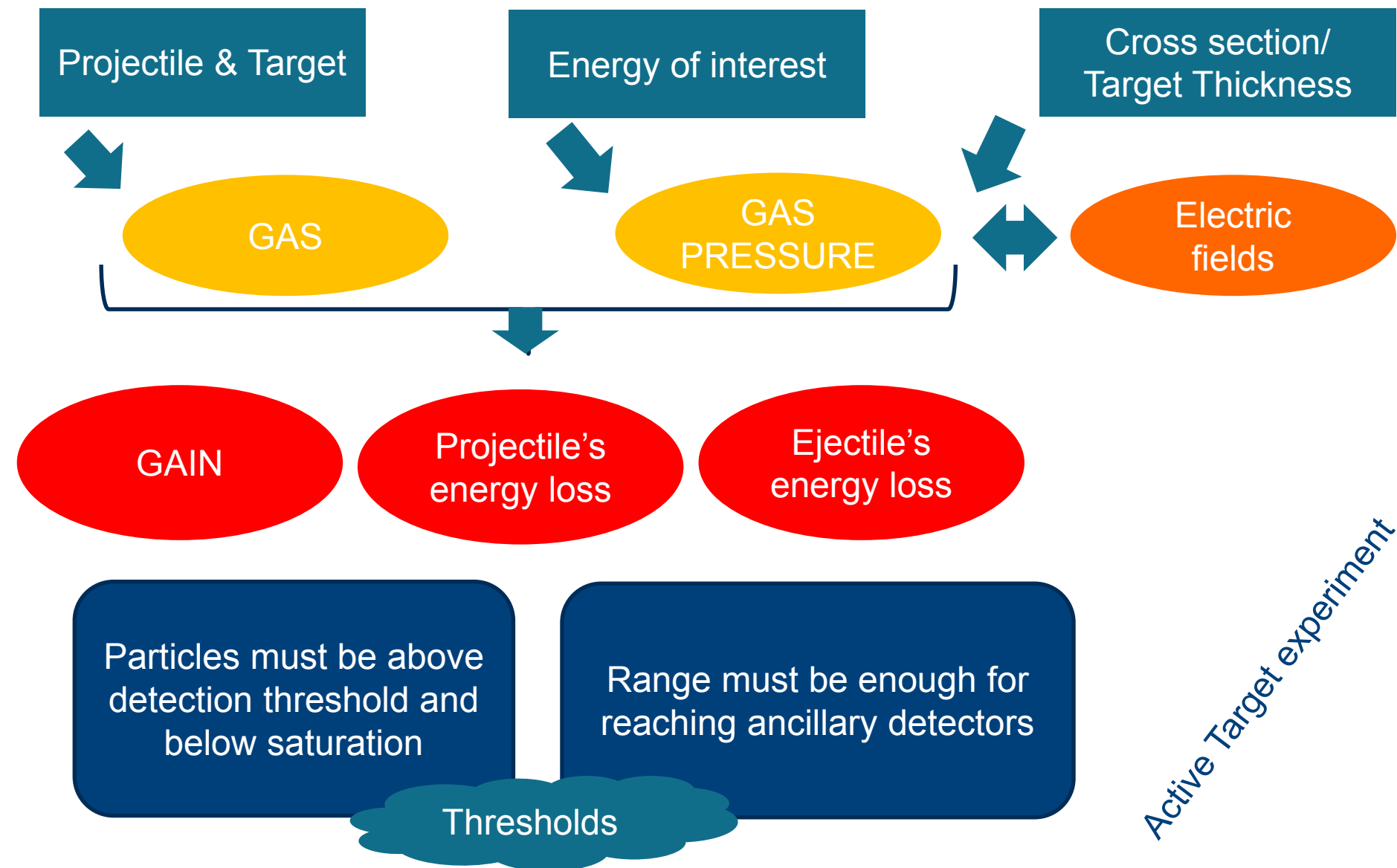
Particles must be above
detection threshold and
below saturation

Range must be enough for
reaching ancillary detectors

Thresholds

Standard experiment

NOTES for experiment's preparation



Summary and outlook

- ACTAR TPC Demonstrator is being exploited for further R&D and for experiments with stable beams
- ACTAR-test campaign at LNS in progress (December 2018 - February 2019): energy loss measurements + direct reactions
- 3 approved experiments at LNS for 2019 (caveat: using pure D₂)
- A path is defined towards an Active Target at SPES

*Takeaway message:
a wide spectrum of opportunities, but not everything is feasible*

ACTAR TPC and NUCLEX collaborations

H. Alvarez-Pol⁶, P. Ascher⁷, M. Babo^{2,8}, S. Barlini⁹, B. Bastin³, M. Bini⁹, B. Blank⁷, M. Bruno¹⁰, M. Caamaño⁶, G. Casini⁹, A. Camaiani⁹, A. Chbihi³, S. Ceruti², G. Collazuol^{11,12}, M. Cinausero¹, D. Dell'Aquila¹⁵, D. Fabris¹¹, M. D'Agostino¹⁰, F. de Oliveira Santos³, N. de Sereville⁸, H. De Witte², B. Duclos³, Q. Fable³, B. Fernandez-Dominguez⁶, F. Flavigny⁸, A. Gottardo¹, M. Gerbaux⁷, J. Giovinazzo⁷, T. Goigoux⁷, F. Gramegna¹, S. Grévy⁷, G.F. Grinyer⁴, J. Grinyer⁴, D. Gruyer¹⁶, F. Hammache⁸, T. Kurtukian-Nieto², B. Mauss³, M. Mazzocco^{11,12}, D. Mengoni^{11,12}, I. Lombardo⁵, L. Morelli^{3,10}, P. Morfouace³, P. Ottanelli⁹, G. Pasquali⁹, J. Pancin³, S. Piantelli⁹, J. Pibernat², E.C. Pollacco¹³, O. Poleshchuk², R. Raabe², J. Refsgaard², T. Roger³, M. Renaud², A.A. Raj², F. Saillant³, P. Sizun¹³, I. Stefan⁸, D. Suzuki¹⁴, J.J. Valiente-Dobòn¹, S. Valdrè⁹, G. Verde⁵, G. Wittwer³, J. Yang².

¹INFN, Laboratori Nazionali di Legnaro, Viale Dell'Università, 2 – 35020 Legnaro (PD), Italy • ²KU Leuven, Instituut voor Kern- en Stralingsfysica, Celestijnenlaan 200D, 3001 Leuven, Belgium • ³GANIL, CEA/DRF-CNRS/IN2P3, Bvd Henri Becquerel, 14076 Caen, France • ⁴Univ of Regina, Regina, Canada • ⁵INFN, Sezione di Catania, Catania, Italy • ⁶Universidade de Santiago de Compostela, 15706 Santiago de Compostela, Spain • ⁷CENBG, Université Bordeaux 1, CNRS/IN2P3, Chemin de Solarium, 33175 Gradignan, France • ⁸IPN Orsay, CNRS/IN2P3, Université Paris-Sud, Université Paris-Saclay, 91406 Orsay, France • ⁹INFN, Sezione di Firenze and Università di Firenze, Firenze, Italy • ¹⁰INFN, Sezione di Bologna and Physics and Astronomy department, University of Bologna, Bologna, Italy • ¹¹INFN, Sezione di Padova, Padova, Italy • ¹²Dipartimento di fisica e Astronomia dell'Università di Padova, Via Marzolo 8, Padova, Italy • ¹³CEA, Centre de Saclay, IRFU/SPhN 91191 Gif-sur-Yvette, France • ¹⁴RIKEN Nishina Center, 2-1 Hirosawa, Wako, Saitama 351-0198, Japan • ¹⁵National Superconducting Cyclotron Laboratory, Michigan State University, East Lansing, Michigan 48824, USA • ¹⁶Laboratoire de Physique Corpusculaire de Caen, 6 Bvd du maréchal Juin 14050 CAEN CEDEX 4, France.